Robotica (2005) volume 23, pp. 1–11. © 2005 Cambridge University Press
DOI: 10.1017/S0263574704000591 Printed in the United Kingdom

Compensatory motion control for a biped walking robot

Hun-ok Lim* and Atsuo Takanishi†

(Received in Final Form: May 24, 2004)

SUMMARY

This paper addresses a compensatory motion control algorithm of a biped robot to deal with stable dynamic walking on even or uneven terrain. This control algorithm consists of three main parts; the introduction of a virtual plane to consider ZMP (Zero Moment Point); an iteration algorithm to compute the trunk motion; and a program control to realize dynamic walking. The virtual plane is defined as a plane formed by the support points between the surface of terrain and the soles. In order to obtain the trunk motion capable of compensating for the moments produced by the motion of the lower-limbs during the walking, ZMP equation on the virtual plane is computed by using an iteration method. Also, a walking pattern is presented which is composed of the trajectories of lower-limbs, waist and trunk. The walking pattern is commanded to the joints of WL-12RIII (Waseda Leg-Twelve Refined Three) using a program control method. Through walking simulations and experiments on an uneven terrain, such as stairs and sloped terrain, the effectiveness of the control method is verified.

KEYWORDS: Virtual plane; Support polygon; Compensatory motion; Walking pattern; ZMP trajectory.

1. INTRODUCTION

Humans and animals use their legs to move with great mobility, but we do not yet have a full understanding of how they do so. One sign of our ignorance is the lack of man-made robots that use legs to obtain high mobility. In this research, our goal is to understand the control of biped robots on an even or uneven terrain. Another goal is to build a useful biped robot that is able to walk in the human living environments.

Recently, the analysis, design, construction and control of biped robots on a level terrain have been studied. Vukobratovic and his co-workers[1] modeled a walking biped robot that was balanced by manipulating the projected center of gravity and the support area provided by the feet. Takanishi and co-workers[2,3] developed the biped walking robot called WL-10RD (Waseda Leg-Ten Revised D) and proposed the sequence control method. Using the control approach, the complete dynamic walking was realized with a walking speed of 1.3 s/step on a flat ground. Raibert and his co-workers[4] built one-, two, and four legged hydraulically actuated robots, based on prismatic compliant legs, and developed three control methods such as the forward velocity, body attitude and hopping height control methods. Hemami and his co-workers[5,6] developed the model of a five link planar biped robot. The model was controlled by using the state feedback. The reference positions and velocities were obtained from the movement of human walking. McGeer[7] studied a passive dynamic running biped robot without a torso where two legs were connected via a spring, and implemented passive walking machines driven only by gravity. Miura and Shimoyama[8] have built a number of small electrically powered walking bipeds that balance using tabular control schemes. Furusho and Masubuchi[9] proposed a hierarchical control strategy to realize the continuous dynamic walking of a five link biped walking robot. Pratt *et al.*[10] described the virtual model control method to control the planar biped robot. This method did not use dynamic inversion to alter the behavior of the biped robot.

Other researchers have studied walking control algorithms to deal with rough terrain. Zheng and Shen[11] proposed a control method for walking on a sloped terrain. Kajita and Tani[12] developed the linear inverted pendulum mode that is based on a massless leg model, to control a biped walking on ground constituted of planes and vertical steps. The biped walking robot with the feet adapting to unleveled surfaces was studied by Yamaguchi *et al.*,[13] which could absorb contact forces produced between its feet and ground. Honda's humanoid robot called P2 showed the ability to walk forward, backward, right, left and up and down on stairs[14]. To date, almost all control methods have used, based on only the motion of the lower-limbs, not the trunk motion.

The adaptability of terrain can be regarded as one of the crucial abilities for biped walking robots to deal with a rough terrain. In the case of a biped walking machine without a trunk which consists of only the lower-limbs, the lower-limbs have to perform two functions at the same time. One is a path control of the lower-limbs according to the surface of terrain. The other is balance control to prevent collapse. In order to achieve dynamic biped walking, the function for stability should take priority over the function for the path control of the lower-limbs. Therefore, the terrain adaptability of this kind of biped robot is severely limited. If the biped robot has a trunk, the functions can be separated. Its trunk carries out the function for stability, while its lower-limbs work out the function for the path control. So, we believe that a biped

* Corresponding author. Department of System Design Engineering, Kanagawa Institute of Technology, 1030 Shimoogino, Atsugi, Kanagawa, 243-0293 Japan, Humanoid Robotics Institute, Waseda University, 3-4-1 Ookubo, Shinjuku, Tokyo, 169-8555 Japan, E-mail: holim@sd.kanagawa-it.ac.jp
† Department of Mechanical Engineering, Waseda University, Humanoid Robotics Institute, Waseda University, Tokyo/Japan.

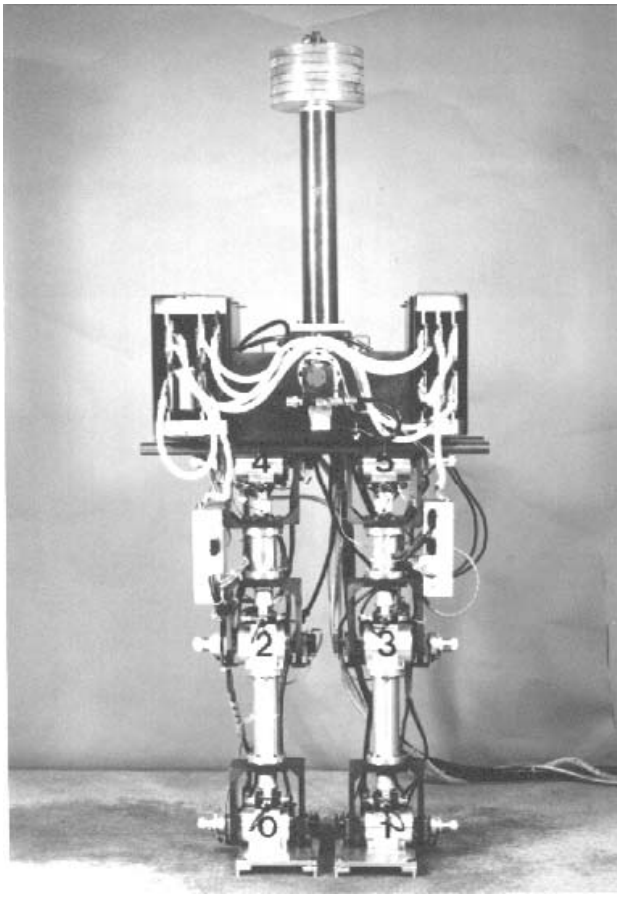

Fig. 1. A biped walking robot WL-12RIII.

walking robot with a trunk will be able to deal with various terrains.

In this paper, we focus on a compensatory motion control that cancels the moments generated by the motion of the lower-limbs. This control method is composed of three main parts: Firstly, a virtual plane is introduced into the surface of terrain to consider ZMP. Secondly, the compensatory motion of the trunk is computed using the motion of the lower-limbs and the ZMP planned on the virtual plane. Finally, a program control is introduced into the WL-12RIII, based on a preset complete walking pattern consisting of the motions of the lower-limbs, waist and trunk. To confirm the control method, we have constructed a biped walking robot having a trunk called WL-12RIII that has eight mechanical degrees of freedom. Its height is about 1.6 m and its weight is 103 kg. A picture of WL-12RIII is shown in Figure 1. Using WL-12RIII, dynamic walking is realized on an even or uneven terrain.

This paper is organized as follows: Section 2 describes how to determine the trajectory of the lower-limbs. Section 3 discusses virtual planes to consider the ZMP concept on an even or uneven terrain. Section 4 describes a compensatory motion control algorithm for moment compensation. Section 5 illustrates an experimental setup and shows experimental results. Finally, conclusions are discussed in Section 6.

2. LEG MOTION PATTERN

Three walking phases are considered to make up the pattern of the lower-limbs, which consists of a double support, a swing and a contact phase. During the swing phase, one foot is not constrained from the ground, while the other foot is on the ground. As soon as the heel of the swing foot reaches the ground, the swing phase is changed to the contact phase. If the toe and heel of the swing foot contacts the ground, the phase becomes the double support phase. Figure 2 shows three walking phases.

In the contact and double support phase, a foot motion pattern on uneven terrain is produced by using a quintic polynomial considering angle, angular velocity, angular acceleration. In the swing phase, a foot motion pattern $\boldsymbol{x}_s$ on an uneven terrain is generated by using a sixth order polynomial, considering the angle, angular velocity, angular acceleration and angle at a half point of the swing phase.

In order to produce a smooth motion of the foot in the swing phase, three constraints arise from the selection of initial, intermediate and final values:

$$\boldsymbol{x}_s(t_0) = \boldsymbol{x}_{s0}, \quad \boldsymbol{x}_s(t_m) = \boldsymbol{x}_{sm}, \quad \boldsymbol{x}_s(t_f) = \boldsymbol{x}_{sf}, \tag{1}$$

$\boldsymbol{x}_s$ have an additional four constraints that are the zero initial and final velocity and acceleration:

$$\dot{\boldsymbol{x}}_s(t_0) = \boldsymbol{0}, \quad \dot{\boldsymbol{x}}_s(t_f) = \boldsymbol{0}, \quad \ddot{\boldsymbol{x}}_s(t_0) = \boldsymbol{0}, \quad \ddot{\boldsymbol{x}}_s(t_f) = \boldsymbol{0}. \tag{2}$$

Since the sixth order polynomial has seven coefficients, it can be made to satisfy the seven constraints given by Equation (1) and Equation (2). These constraints uniquely specify the following equation:

$$\boldsymbol{x}_s(t) = \boldsymbol{c}_0 + \boldsymbol{c}_1 t + \boldsymbol{c}_2 t^2 + \boldsymbol{c}_3 t^3 + \boldsymbol{c}_4 t^4 + \boldsymbol{c}_5 t^5 + \boldsymbol{c}_6 t^6. \tag{3}$$

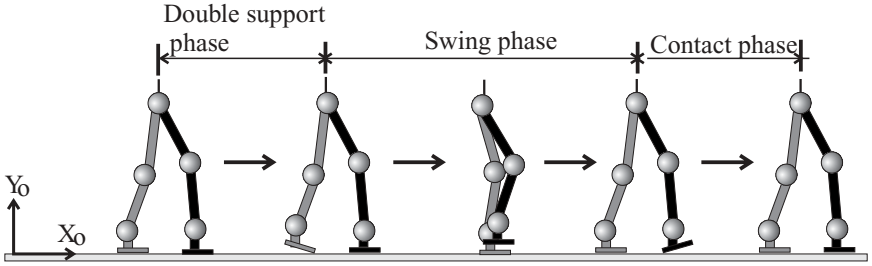

Fig. 2. Three walking phases.

https://doi.org/10.1017/S0263574704000591 Published online by Cambridge University Press

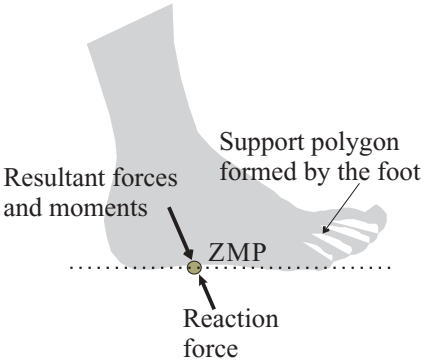

Fig. 3. ZMP under the sole. A support polygon made between the sole and the ground.

Also, the velocity and acceleration along this trajectory are as follows:

$$\dot{\boldsymbol{x}}_s(t) = \boldsymbol{c}_1 + 2\boldsymbol{c}_2 t + 3\boldsymbol{c}_3 t^2 + 4\boldsymbol{c}_4 t^3 + 5\boldsymbol{c}_5 t^4 + 6\boldsymbol{c}_6 t^5,$$
$$\ddot{\boldsymbol{x}}_s(t) = 2\boldsymbol{c}_2 + 6\boldsymbol{c}_3 t + 12\boldsymbol{c}_4 t^2 + 20\boldsymbol{c}_5 t^3 + 30\boldsymbol{c}_6 t^4. \quad (4)$$

Combining Equation (3) and Equation (4) with the seven constraints, the seven coefficients can be obtained. Then, substituting these coefficients for Equation (3), the foot pattern will be obtained. Also, a waist pattern is set by a polynomial, considering the movable range of the legs. In addition, a knee pattern is geometrically computed on the basis of the foot and waist pattern.

3. VIRTUAL PLANE AND ZMP TRAJECTORY

In this section, a virtual plane is discussed to calculate ZMP (Zero Moment Point). Also, a preset ZMP trajectory is described for a moment compensation motion.

3.1. Virtual plane

The ZMP (Zero Moment Point) concept is used for stability. Consider a single support phase in which one foot is not constrained from the ground, while the other is on the ground. As shown in Figure 3, the support polygon (stable region) is made by the contact points between the sole of the foot and the ground. To maintain the dynamic equilibrium of a biped walking robot, the ground reaction force should act at an appropriate point on the foot sole to balance all the forces and moments acting on its whole body. This means that ZMP exists at a point where the total forces and moments are equal to zero in the support polygon.[1]

To consider ZMP on uneven terrain, virtual planes are defined according to the terrain's geometry. At the first stage of this study, a sagittal and a latteral plane formed between the terrain's surface and the soles of the feet are regarded as a virtual plane, as shown in Figure 4. For mathematical quantities, virtual coordinate frames should be fixed on the virtual planes.

In case of the single support phase, the virtual plane S_1 is formed by the projection of the hind toe and heel on the ground, as shown in Figure 4(a). In the contact phase, the virtual plane S_2 is defined by the fore heel and the hind foot,

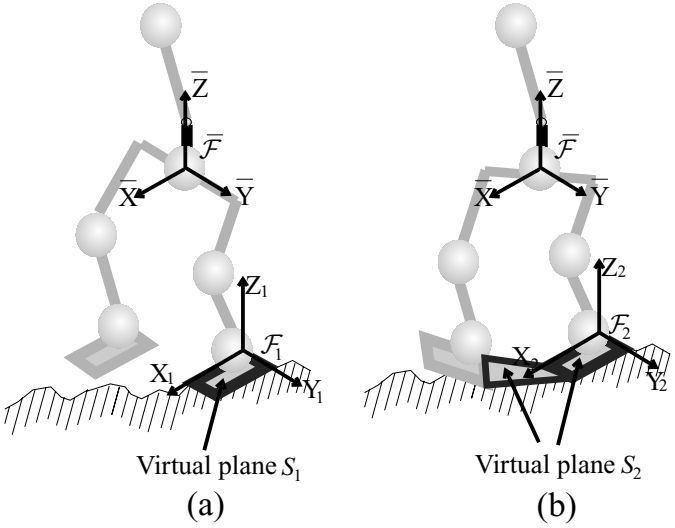

Fig. 4. Virtual planes and frames: (a) Virtual frame $\mathcal{F}_1$ fixed on the virtual plane S_1 and (b) Virtual frame $\mathcal{F}_2$ fixed on the virtual plane S_2.

as shown in Figure 4(2). Also, the virtual plane is made between the fore and hind foot in the double support phase. These virtual planes are formed along the walking path as well as the number of the step.

3.2. ZMP trajectory

In order to calculate the compensatory motion of the trunk, ZMP trajectory is arbitrarily desired in the stable region formed according to a foot length and a step length. Figure 5 shows the examples of the X and Y time ZMP trajectories, $\bar{X}^p_{zmp}$ and $\bar{Y}^p_{zmp}$, planned in the virtual planes such as planes A, B, C and so on. In the double support phase, we consider the stable region of 0.2 m × 0.38 m excepting the step length, while in the single support phase, the stable region of 0.2 m × 0.17 m.

4. COMPENSATORY MOTION CONTROL

In this section, compensatory motion control is discussed which can cancel the moments produced by the movement of a biped robot.

4.1. ZMP equation on virtual plane

In modeling a biped walking robot, five assumptions are defined as follows:

(i) The walking robot consists of a set of particles.
(ii) The foothold of the robot is rigid and not moved by any force and moment.
(iii) The contact region between the foot and the terrain's surface is a set of contact points.
(iv) The coefficients of friction for rotation around the X^k, Y^k and Z^k-axes are nearly zero at a contact point between the feet and the terrain's surface.
(v) The foot of the robot does not slide on the contact surface.

In this study, we don't consider the dynamic motion of the waist center. According to the mass distribution of the biped robot, the moment balance around a contact point p^k

https://doi.org/10.1017/S0263574704000591 Published online by Cambridge University Press

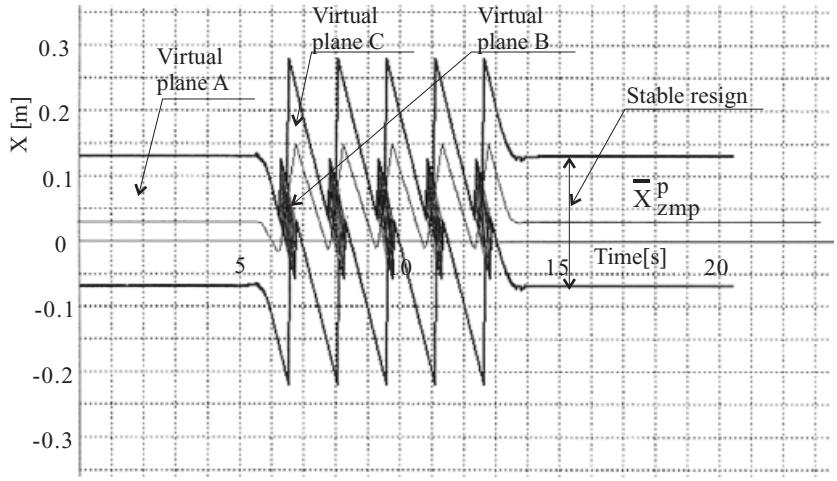

(a) X ZMP trajectory.

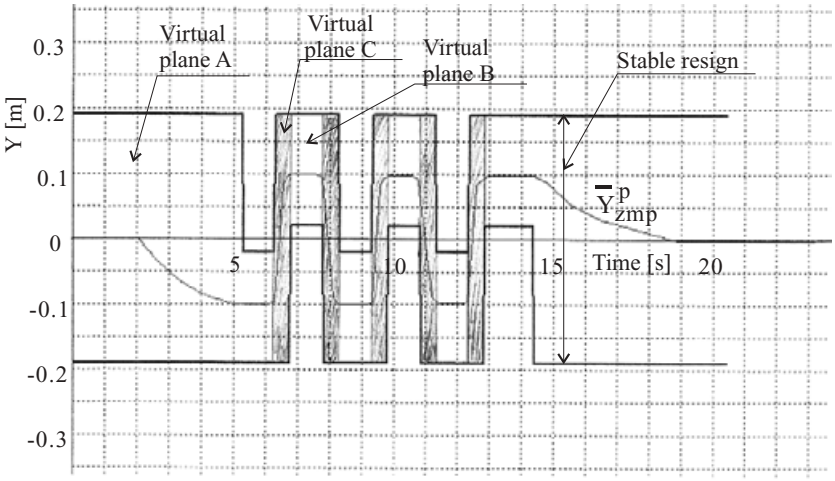

(b) Y ZMP trajectory.

Fig. 5. ZMP trajectories planned in the virtual planes.

on the virtual plane, as shown in Figure 6, can be obtained as follows:

$$\sum_{i=1}^{n} m_i\left(\boldsymbol{r}_i^k - \boldsymbol{r}_p^k\right) \times \left(\left(\ddot{\boldsymbol{r}}_i^k + \boldsymbol{G}^k\right) - \ddot{\boldsymbol{p}}^k\right) + \boldsymbol{T}^k = \boldsymbol{0}, \qquad (5)$$

where m_i is the mass of the particle i. $\boldsymbol{r}_p^k$ is the position vector of the contact point p^k with respect to the virtual coordinate frame $\mathcal{F}_k$. $\boldsymbol{r}_i^k$ and $\ddot{\boldsymbol{r}}_i^k$ denotes the position and acceleration vectors of the particle i with respect to the virtual coordinate frame $\mathcal{F}_k$, respectively. $\boldsymbol{G}^k$ is the gravitational acceleration vector, $\boldsymbol{T}^k$ is the moment acting on the contact point p^k.

Let ZMP be on the point p^k. The moment $\boldsymbol{T}^k$ will be a zero vector by the ZMP concept. Therefore, Equation (5) can be rewritten as

$$X_{zmp}^k = \frac{\sum_{i=1}^n m_i\left(\ddot{z}_i^k + g_z^k\right)x_i^k - \sum_{i=1}^n m_i\left(\ddot{x}_i^k + g_x^k\right)z_i^k}{\sum_{i=1}^n m_i\left(\ddot{z}_i^k + g_z^k\right)},$$
$$Y_{zmp}^k = \frac{\sum_{i=1}^n m_i\left(\ddot{z}_i^k + g_z^k\right)y_i^k - \sum_{i=1}^n m_i\left(\ddot{y}_i^k + g_y^k\right)z_i^k}{\sum_{i=1}^n m_i\left(\ddot{z}_i^k + g_z^k\right)}. \qquad (6)$$

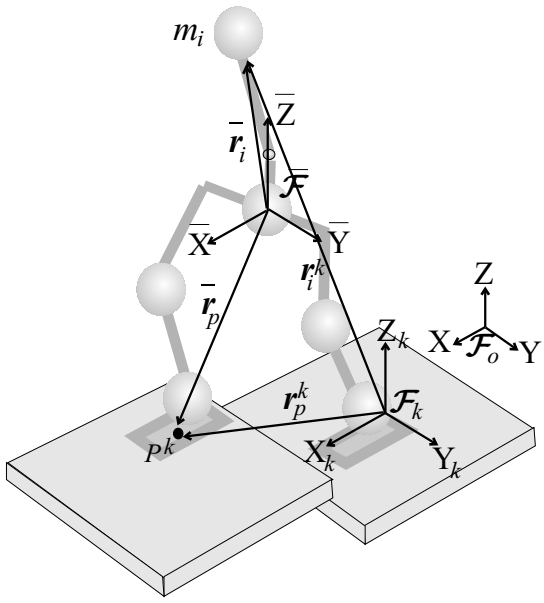

Fig. 6. Coordinate frames.

https://doi.org/10.1017/S0263574704000591 Published online by Cambridge University Press

4.2. Linearization

In order to obtain the trunk motion from Equation (6) derived on the uneven terrain, we assume the biped model walks on a horizontal plane. A world coordinate frame $\mathcal{F}_o$ is fixed on the horizontal plane where the robot can walk (Figure 6). Also, a waist coordinate frame $\bar{\mathcal{F}}$ is attached on the center of the waist to consider the relative motion of each particle. ZMP equations, $\bar{X}_{zmp}$ and $\bar{Y}_{zmp}$, can be written with respect to the $\bar{\mathcal{F}}$ as follow:

$$\bar{X}_{zmp} = \frac{N_x}{D}, \qquad \bar{Y}_{zmp} = \frac{N_y}{D}, \tag{7}$$

where

$$\begin{aligned} N_x &= \sum_{i=1}^{n} m_i(\ddot{\bar{z}}_i + \ddot{z}_q + g_z)(\bar{x}_i + z_q) \\ &\quad - \sum_{i=1}^{n} m_i(\ddot{\bar{x}}_i + \ddot{x}_q + g_x)(\bar{z}_i + z_q), \\ N_y &= \sum_{i=1}^{n} m_i(\ddot{\bar{z}}_i + \ddot{z}_q + g_z)(\bar{y}_i + y_q) \\ &\quad - \sum_{i=1}^{n} m_i(\ddot{\bar{y}}_i + \ddot{y}_q + g_y)(\bar{z}_i + z_q), \\ D &= \sum_{i=1}^{n} m_i(\ddot{\bar{z}}_i + \ddot{z}_q + g_z), \end{aligned} \tag{8}$$

where $\bar{x}_i$, $\bar{y}_i$ and $\bar{z}_i$ are the positions of joints of the biped relative to the $\bar{\mathcal{F}}$. $\bar{x}_q$, $\bar{y}_q$ and $\bar{z}_q$ are the positions of the origin of $\bar{\mathcal{F}}$ from the origin of $\mathcal{F}$, respectively.

If the terms about the motion of the trunk particle in Equation (7) are put on the right-hand as unknown variables, and the terms about the motion of the lower-limb particles are put on the left-hand as known variables, $K_x(t)$ and $K_y(t)$, the equations of the trunk motion can be rewritten as

$$\begin{aligned} K_x(t) &= \ddot{\bar{z}}_t(\ddot{x}_q + g_x) + \ddot{\bar{z}}_t\bar{X}_{zmp} + (\bar{z}_t + z_q)\ddot{x}_t \\ &\quad - (\ddot{\bar{z}}_t + \ddot{z}_q + g_z)\bar{x}_t, \end{aligned} \tag{9}$$

$$\begin{aligned} K_y(t) &= \ddot{\bar{z}}_t(\ddot{y}_q + g_y) + \ddot{\bar{z}}_t\bar{Y}_{zmp} + (\bar{z}_t + z_q)\ddot{y}_t \\ &\quad - (\ddot{\bar{z}}_t + \ddot{z}_q + g_z)\bar{y}_t, \end{aligned} \tag{10}$$

where $\bar{x}_t$, $\bar{y}_t$ and $\bar{z}_t$ are the positions of trunk with respect to the $\bar{\mathcal{F}}$.

These equations, however, are interferential and non-linear because each equation has the same variable $\bar{z}_t$, and the trunk is connected to the lower-limbs through rotational joints. Therefore, it is difficult to derive analytic solutions from the equations. We assume that the trunk particle m_t does not move vertically, as shown in Figure 7.

$$\ddot{\bar{z}}_t = 0, \qquad z_q = const., \qquad \bar{z}_t + z_q = const. \tag{11}$$

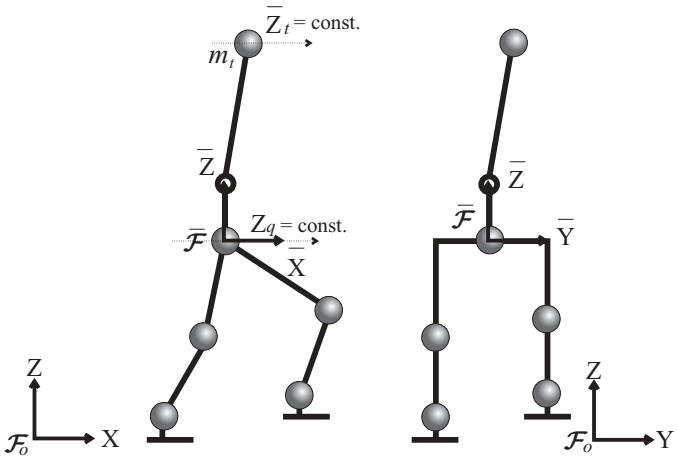

Fig. 7. Linearized model.

Thus, the decoupled linear differential equations are as follows:

$$\begin{aligned} \Phi(t) &= (\bar{z}_t + z_q)\ddot{\bar{x}}_t - g_z\bar{x}_t, \\ \Psi(t) &= (\bar{z}_t + z_q)\ddot{\bar{y}}_t - g_z\bar{y}_t, \end{aligned} \tag{12}$$

where

$$\begin{aligned} \Phi(t) &= K_x(t) - \bar{z}_t\ddot{x}_q - \bar{z}_t g_x \\ \Psi(t) &= K_y(t) - \bar{z}_t\ddot{y}_q - \bar{z}_t g_y. \end{aligned} \tag{13}$$

The solutions derived from Equation (12) do not converge because the roots of characteristic equations of Equation (12) are non-negative real numbers. In case of steady walking, the trajectories of the lower-limbs and the ZMP can be planned periodically relative to the waist frame $\bar{\mathcal{F}}$. If $\Phi(t)$ and $\Psi(t)$ are known periodic functions, the equations have periodic solutions as particular solutions. So, we can easily get approximate periodic solutions using FFT (Fast Fourier Transformation).[15]

4.3. Strict compensatory motion

The approximate solutions derived from Equation (12) are effective when the trunk is quite long and the walking speed is relatively slow compared to that of a human. To obtain strict periodic solutions of ZMP Equation (6), an iteration method is employed. Firstly, we project the ZMP planned on the virtual plane onto the horizontal plane formed by the X and Y axes of world frame $\mathcal{F}_o$ and substitute the projected ZMP into the decoupled linear Equation (12). As a result, the approximate periodic motions of the trunk, $\bar{x}_t$ and $\bar{y}_t$, are derived. Secondly, we substitute both the lower-limb motion and the approximate trunk motion into the ZMP Equation (6), and calculate the ZMP relative to the waist frame, $\bar{X}^{kc}_{zmp}$ and $\bar{Y}^{kc}_{zmp}$. Then, we compute the ZMP errors between the calculated ZMP and planned ZMP as

$$e_x = \bar{X}^{p}_{zmp} - \bar{X}^{kc}_{zmp}, \quad e_y = \bar{Y}^{p}_{zmp} - \bar{Y}^{kc}_{zmp}. \tag{14}$$

https://doi.org/10.1017/S0263574704000591 Published online by Cambridge University Press

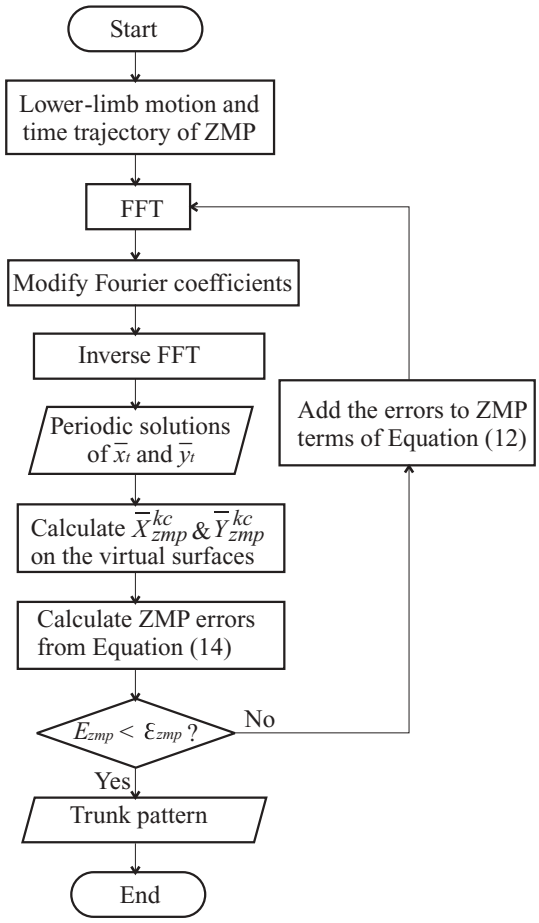

Fig. 8. Block diagram to calculate trunk motion.

Finally, these errors are added to the ZMP terms of linear Equation (12), and the approximate periodic solutions are calculated again. This operation is repeated until the errors fall under certain tolerance levels. This algorithm is applicable to not only the steady walking but also the complete walking. A block diagram of the iteration algorithm is shown in Figure 8.

4.4. Trunk motion simulation

We have numerically verified the convergence of the solutions. In simulation, two parameters are considered: the length of the trunk and the walking speed. We can see that the errors of the ZMP drop below 1.0 mm after 10 iteration times, as shown in Figures 9 and 10.

Consider only the motion of the trunk around the pitch axis to investigate the compensatory motion. The transfer function in the frequency domain between the trunk motion $\bar{y}_t$ and the leg motion $\Phi(t)$ of Equation (12), $\bar{y}_t(\omega)$, can be expressed as

$$\bar{y}_t(\omega) = \frac{2p}{\omega^2 + p^2} q = \left(\frac{1}{p - j\omega} + \frac{1}{p + j\omega} \right) q, \quad (15)$$

where

$$p = \sqrt{\frac{g_z}{\bar{z}_t - \bar{z}_{zmp}}}, \qquad q = -\frac{1}{2g_z} \sqrt{\frac{g_z}{\bar{z}_t - \bar{z}_{zmp}}}. \quad (16)$$

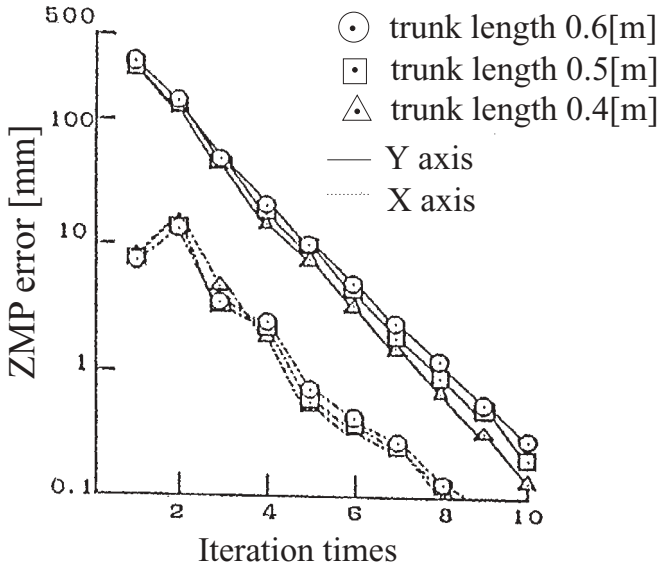

Fig. 9. Convergence of iteration solutions. When the walking speed is 2.6 s/step, the trunk length is changed.

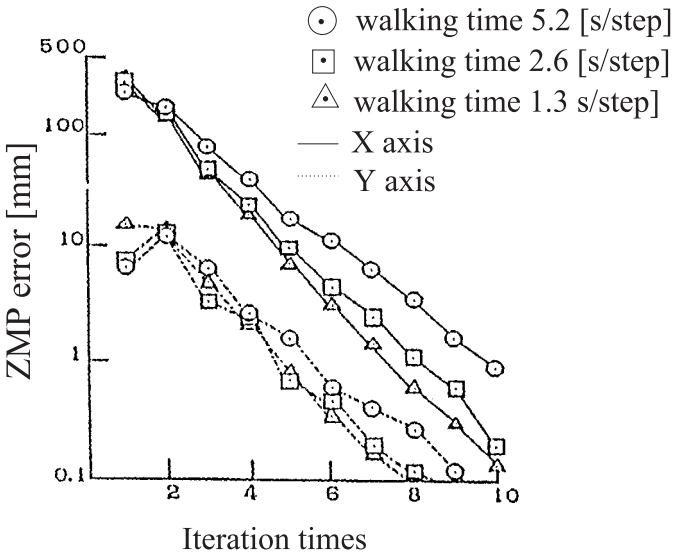

Fig. 10. Convergence of iteration solutions. When the trunk length is 0.6 m, the walking speed is changed.

Equation (15) is generally known as the Lorentz function, and its primitive function is written as

$$\bar{y}_t(t) = q e^{-p|t|}. \quad (17)$$

We can imagine from Equation (17) that the casual law may not be applied anymore. If the walking speed of the biped robot is increased, it goes without saying that $\bar{y}_t(t)$ affects stability more badly. The trunk, therefore, should be in motion earlier than the shift of ZMP on the floor to cancel the effect of the produced moments.

The relationship between the trunk motion and the applied force has been simulated. When a biped robot is not in motion, an impulse moment 1000 Nm is applied to the pitch trunk. Figure 11 shows the pitch motion of the trunk. In this

https://doi.org/10.1017/S0263574704000591 Published online by Cambridge University Press

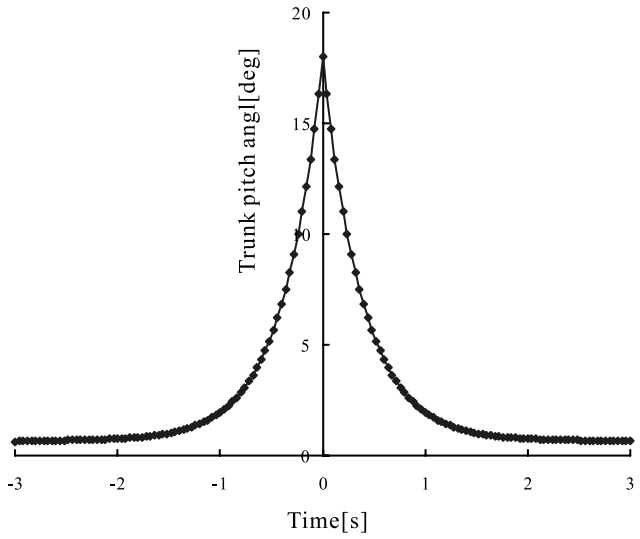

Fig. 11. Compensatory motion of the trunk.

simulation, we can see that the compensatory motion of the trunk should be begun with a view of balancing before and after the impulse moment is applied to the biped robot.

4.5. Complete walking pattern

On the basis of the trajectories of the leg and the trunk, each joint angle is calculated by inverse kinematics. Then, a complete walking pattern is made as CSV (Comma separated values). The walking pattern is commanded to the biped hardware system using the program control already proposed.[3] Figure 12 shows the flowchart of a complete walking pattern.

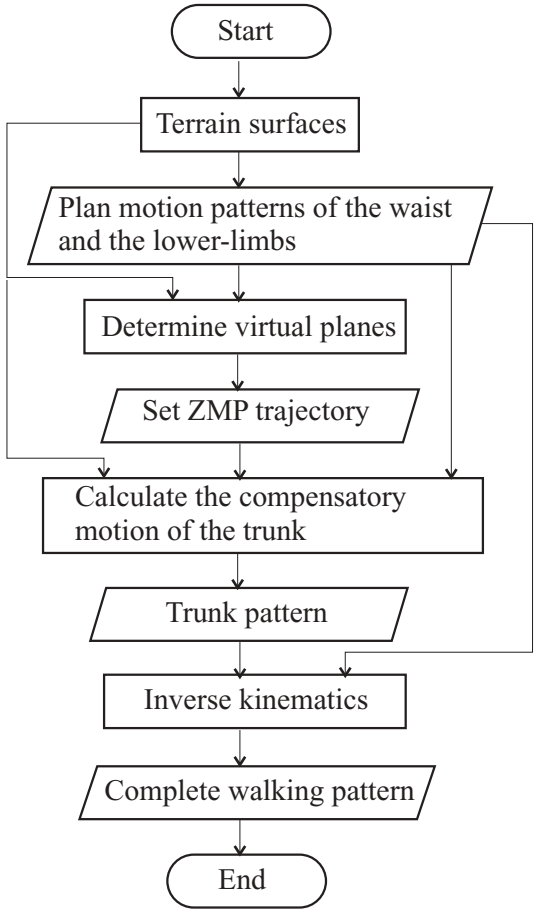

Fig. 12. Complete walking pattern.

5. WALKING EXPERIMENT

In order to confirm the validity of the control method, dynamic walking experiments on planes, stairs and slopes are conducted. In this section, we describe the structure of the experimental system and show the experimental results.

5.1. System description

An eight degrees of freedom biped robot called WL-12RIII has been developed to explore the dynamic walking on an uneven terrain, which consists of lower-limbs and a trunk (see Figure 1). The trunk having two degrees of freedom can bend front-to-back and side-to-side. Each leg has three segments, such as a thigh, shank and sole that are connected through rotational joints to each other. Figure 13 shows the assembly drawing of WL-12RIII. The motion of the waist and lower-limbs is limited by mechanical stoppers and software. The biped robot uses an electro-hydraulic servo system consisting of rotary actuators and a servo valves. The structural frame of the biped is mainly made of CFRP (Carbon Fiber Reinforced Plastic), and the actuators and manifold are made of duralumin. The height of the biped is about 1.6 m and its total weight is 103 kg.

Each actuator is equipped with a potentiometer and a tachometer generator that detect the rotational angle and angular velocity, respectively. The potentiometer and the

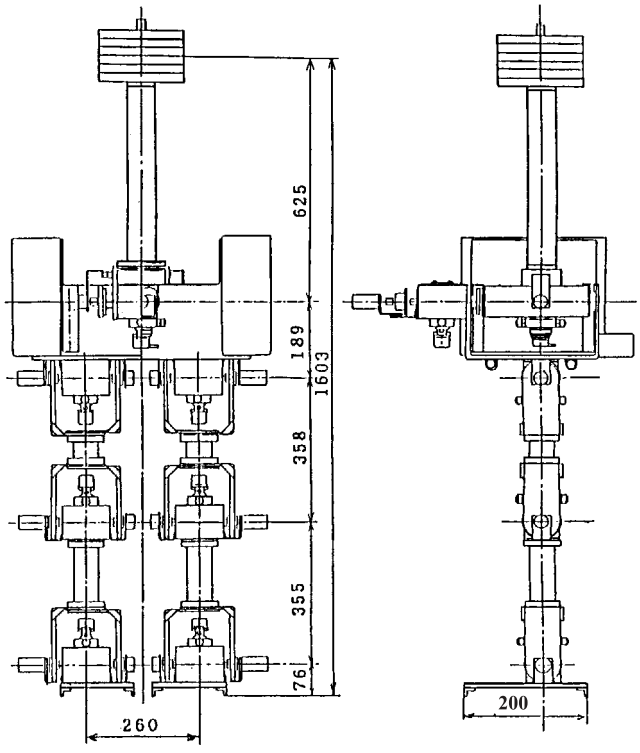

Fig. 13. Assembly drawing of WL-12RIII. The height of the robot is 1.6 m, and the total weight is 103 kg.

https://doi.org/10.1017/S0263574704000591 Published online by Cambridge University Press

Table I. Mass Parameters of WL-12RIII.

Part	Weight kg
Trunk	30.5
Waist (pitch)	5.0
Waist (roll)	5.0
Hip	7.5
Knee	7.0
Ankle	6.5

Table II. Length Parameters of WL-12RIII.

Part	Length mm
Trunk	625
Thigh	358
Shank	355
Sole	200 × 170

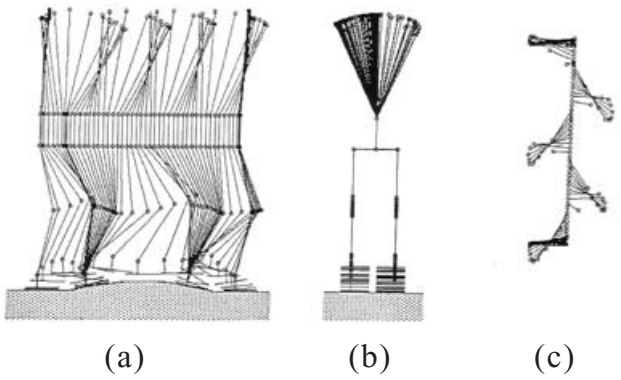

Fig. 14. Walking simulation on the trapezoid floor: (a) sagittal plane, (b) latteral plane, (c) horizontal plane.

tachometer generator are directly connected to the shaft of the actuator to make the feedback control correct and stable. Also, the actuator is equipped with two pressure sensors in the hydraulic circuit; they monitor the output torque. Each sole is equipped with two microswitches that monitor the contact of the toe and heel. The parameters of the WL-12RIII are illustrated in Tables I and II.

All the computations to control WL-12RIII are carried out by the control computer and the control program that is written in *C* and assembly language. The servo rate is 1 kHz. The computer system is mounted on the on the right and left side of the waist.

5.2. Simulation and experimental results

We have conducted dynamic walking experiments on a plane, a trapezoid floor and stairs. The dimension of the staircase is 0.1 m height, 0.4 m width and 0.5 m depth. The trapezoid floor is made by two slopes with 10 deg and a plane. On the staircase, the dynamic complete walking is realized with the step time of 2.6 s/step and the step width of 0.3 m/step. On the other hand, on the trapezoid floor, the dynamic complete walking is realized with the step time of 1.6 s/step and the step width of 0.3 m/step.

WL-12RIII tilts forwards the trunk like a human, going up the slope as shown Figure 14, while it tilts backwards the

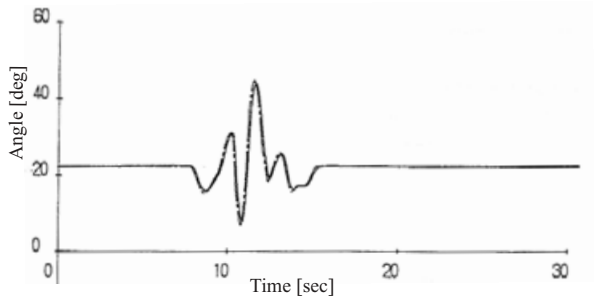

(a) Right ankle angle history.

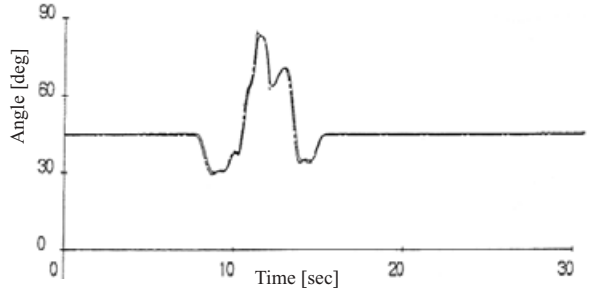

(b) Right knee angle history.

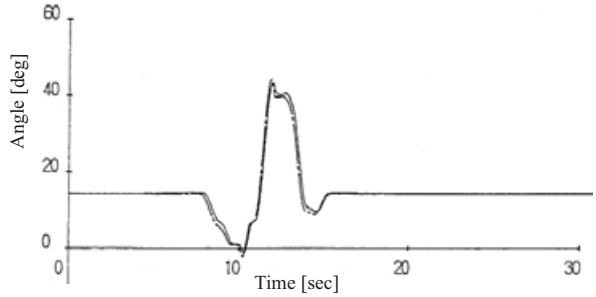

(c) Right hip angle history.

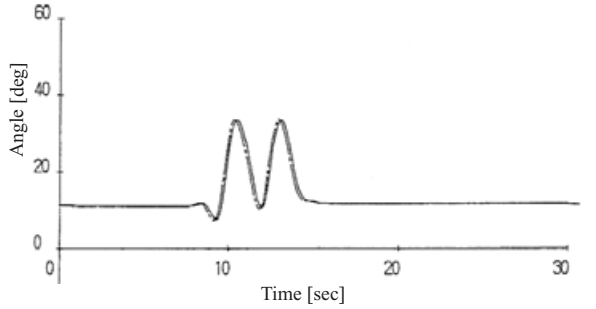

(d) Pitch trunk angle history.

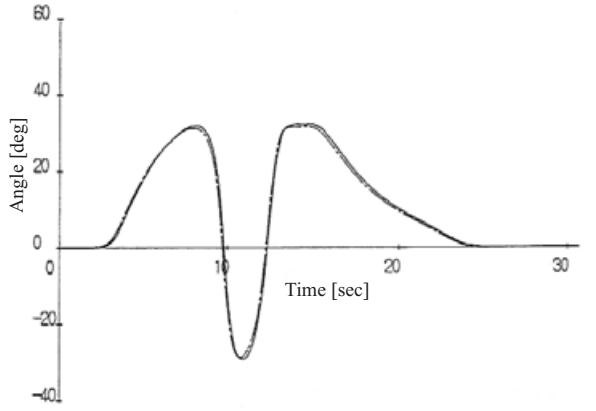

(e) Roll trunk angle history.

Fig. 15. Angle history in an experiment going up the stair. The dotted lines denote desired angles and the solid lines denote response angles.

https://doi.org/10.1017/S0263574704000591 Published online by Cambridge University Press

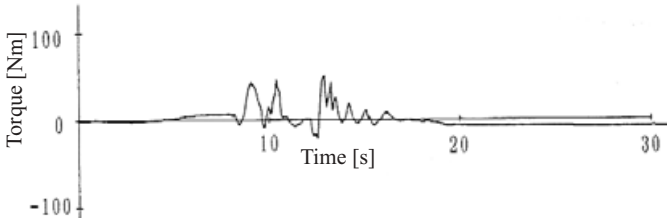

(a) Right ankle torque history.

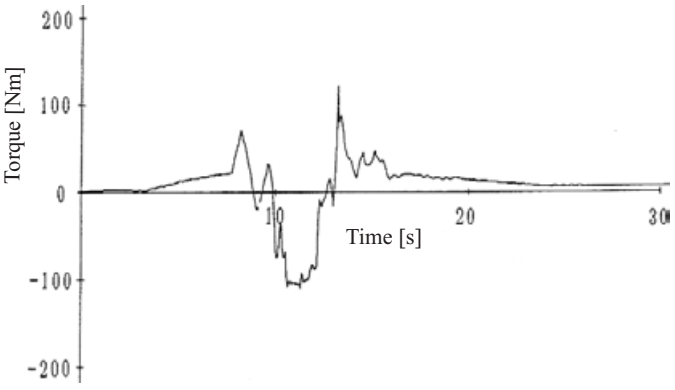

(b) Right knee angle history.

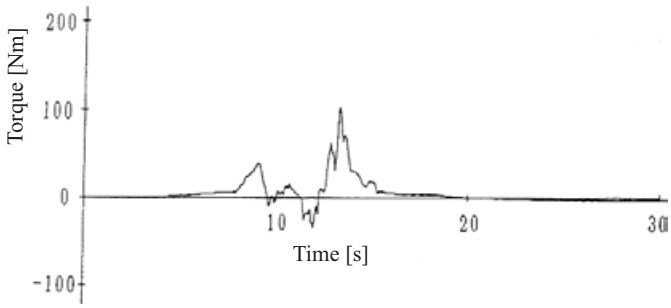

(c) Right hip torque history.

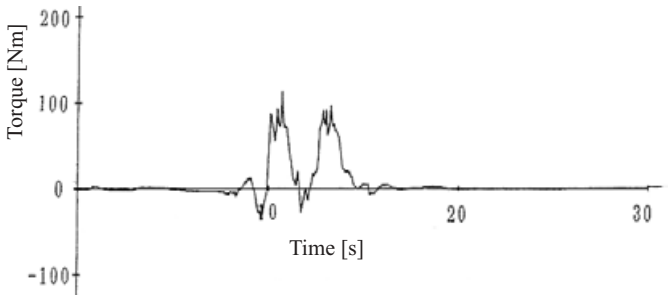

(d) Pitch trunk torque history.

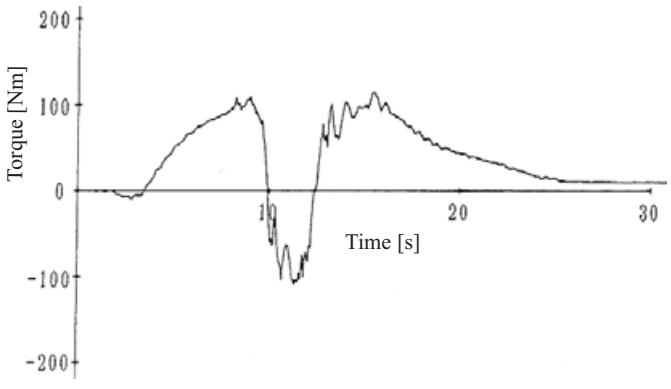

(e) Roll trunk torque history.

Fig. 16. Torque history in an experiment going up the stair. The dotted lines denote desired torques and the solid lines denote response torques.

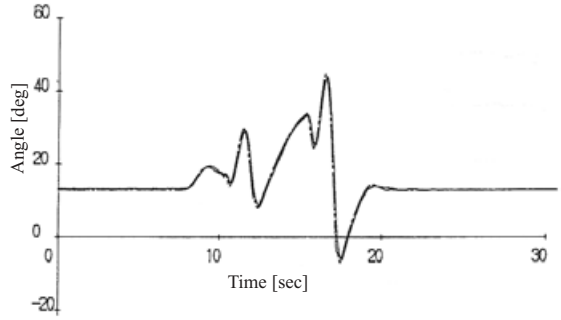

(a) Right ankle angle history.

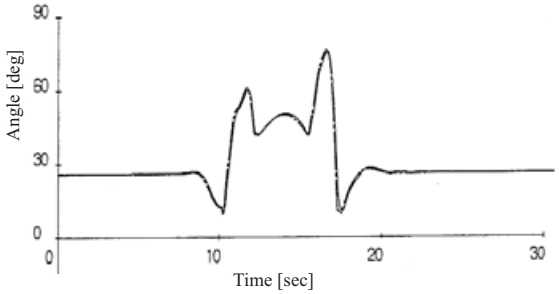

(b) Right knee angle history.

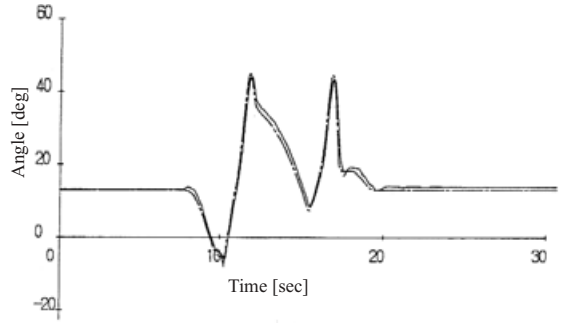

(c) Right hip angle history.

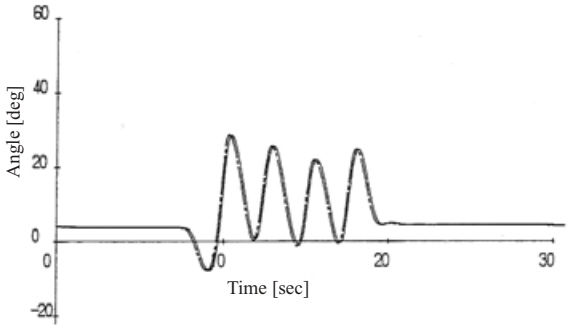

(d) Pitch trunk angle history.

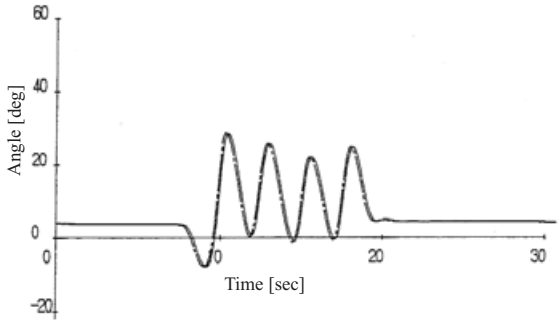

(e) Roll trunk angle history.

Fig. 17. Angle history in an experiment walking on the trapezoid terrain. The dotted lines denote desired angles and the solid lines denote response angles.

https://doi.org/10.1017/S0263574704000591 Published online by Cambridge University Press

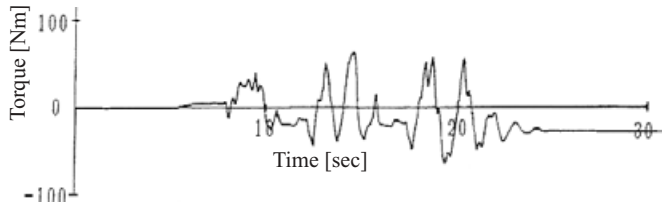

(a) Right ankle torque history.

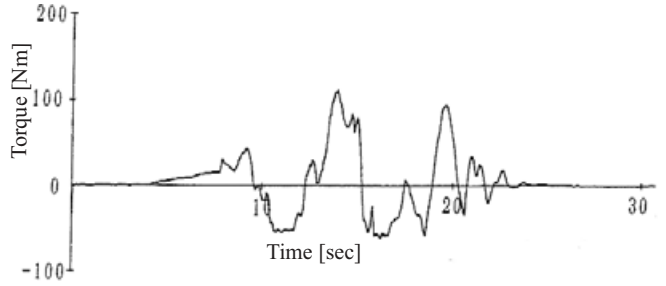

(b) Right knee torque history.

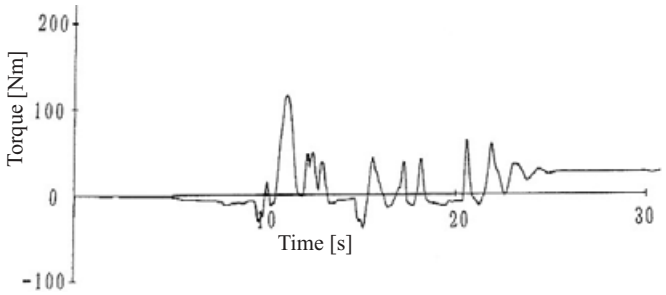

(c) Right hip torque history.

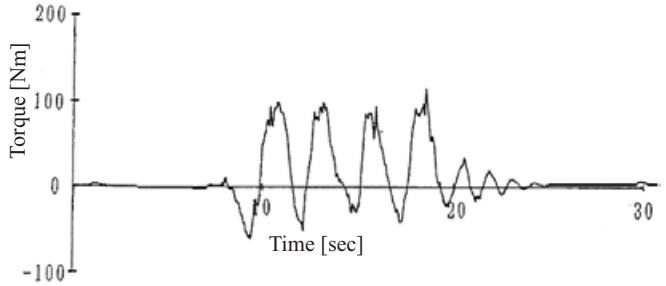

(d) Pitch trunk torque history.

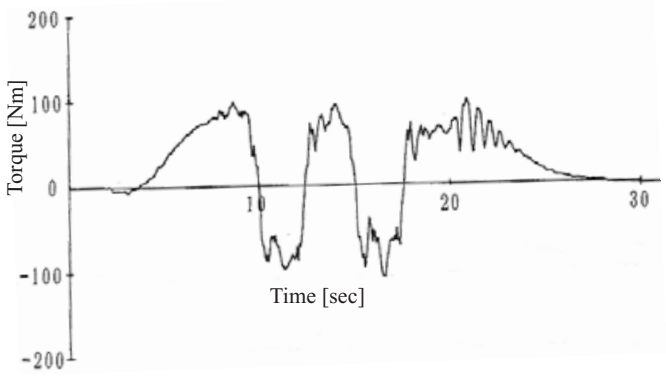

(e) Roll trunk torque history.

Fig. 18. Torque history in an experiment walking on the trapezoid terrain. The dotted lines denote desired torques and the solid lines denote response torques.

trunk, going down the slope. It means that the torque of the knee can be decreased by these trunk motions. In the stance phase, the center of mass is moved from the back to the front, while in the swing phase the center of mass is not moved so much.

An experiment going down a stair with the height of 0.12 m, was not realized because the heel of the fore foot was landed firstly on the stair and the hind ankle joint exceeded the limited maximum angle. However, a human does not bend so much the ankle joint because the toe of the front foot contacts the stair at first suppressing the contact force, and the toe of the back foot moves last. In addition, a human employs well the rotation of the yaw axis of the waist. To realize a human-like walking, the biped robot should have the yaw axis of the waist and the combination motion of the trunk and the waist should be used.

When the biped robot goes up two stairs with three step, the angle and torque response are shown in Figures 15 and 16, respectively. Also, Figures 17 and 18 show the angle and torque response, respectively when the biped robot moves with the same walking pattern (see Figure 14) as the simulation on the trapezoid floor. In experimental results, the dotted lines denote desired values and the solid lines response values.

These response patterns follow very well the desired patterns, excepting some steep change points of angle. The angles are sharply increased or decreased immediately after the swing phase is changed to the stance phase, as shown in Figures 15 and 17. The reason is that the angle patterns are determined using inverse kinematics after the foot and the waist trajectories are smoothly planned with respect to the word coordinate frame. If the biped robot takes more time in the swing phase, these patterns can be made more smoothly. In addition, the torque changes are large at the latter half of the swing phase, as shown in Figures 16 and 18. However, if the biped robot stretches the knee, smaller torques will be able to be generated.

We conducted walking experiments on the trapezoid floor with the step length of 0.3 m and the step time of 1.3 s/step but did not realize dynamic walking. The reason is that the step speed did not decrease enough, and the tilt angle of the floor was different when the foot sole lands on the floor. Also, the contact force was not reduced sufficiently because of the program control based on the complete walking pattern. To reduce the contact force, a compliance control and a torque control are expected to be applied to the robot leg.

These results clarify that the motion of the trunk calculated by the control algorithm is effectively used for the compensation of the moments generated by the motion of the lower-limbs

6. CONCLUSION

To realize dynamic walking on even and uneven terrain, we have proposed a compensatory motion control algorithm. The control algorithm consists of three main parts. Firstly, a virtual plane on the terrain is introduced to consider ZMP, which is formed according to the contact state of the robot feet. Secondly, the compensatory motion of the trunk is calculated using the motion of the lower-limbs and the ZMP

https://doi.org/10.1017/S0263574704000591 Published online by Cambridge University Press

planned on the virtual plane. Finally, a program control is introduced into the WL-12RIII, based on a complete walking pattern consisting of the motions of the lower-limbs, waist and trunk. This algorithm is applicable to not only the steady walking but also the complete walking. Through hardware experiments using the complete walking pattern, the effectiveness of the proposed control approach was verified.

Acknowledgment

The authors would like to thank Kuroda Precision Industries Ltd., Moog Japan Ltd. and Toray Industries Inc. for supporting us in developing the hardware.

References

1. M. Vukobratovic, A. A. Frank and D. Juricic, "On the stability of biped locomotion," *IEEE Trans. of Biomedical Engineering* **17**, No. 1, 25–36 (1970).
2. A. Takanishi, M. Ishida, Y. Yamazaki and I. Kato, "The realization of dynamic walking by the biped walking robot," *Proc. IEEE Int. Conf. Robotics and Automation*, St. Louis, MO (Mar., 1985), pp. 459–466.
3. A. Takanishi, Y. Egusa, M. Tochizawa, T. Takebayashi and I. Kato, "Realization of dynamic walking stabilized with trunk motion," *Proc. CISM-IFToMM Symp. Theory and Practice of Robots and Manipulators* (1988), pp. 68–79.
4. M. H. Raibert, *Legged Robots That Balance* (MIT Press, Cambridge, MA, 1986).
5. R. L. Farnsworth and H. Hemami, "Postural and gait stability of a planar five link biped by simulation," *IEEE Trans. Automatic Control* **22**, No. 3, 452–458 (June, 1977).
6. H. Hemami and B. F. Wyman, "Modeling and control of constrained dynamics systems with application to biped locomotion in the frontal plane," *IEEE Trans. Automatic Control* **24**, 526–535 (1992).
7. T. McGeer, "Passive bipedal walking," *Int. J. Robotics Research* **9**, No. 2, 60–74 (1990).
8. H. Miura and I. Shimoyama, "Dynamic walk of a biped," *Int. J. Robotics Research* **3**, No. 2, 60–74 (Summer, 1984).
9. J. Furusho and M. Masubuchi, "Control of a dynamical biped locomotion system for steady walking," *ASME J. Dynamics Systems, Measurement, and Control* **108**, 111–118 (June, 1986).
10. J. Pratt, P. Dilworth and G. Pratt, "Virtual mode control of a bipedal walking robot," *Proc. IEEE Int. Conf. Robotics and Automation*, Albuquerque, NM (Apr., 1997) pp. 193–198.
11. Y. Zheng and J. Shen, "Gait synthesis for the sd-2 biped robot to climb sloping surface," *IEEE Trans. Robotics and Automation* **6**, No. 1, 86–96 (1990).
12. S. Kajita and K. Tani, "Study of dynamic biped locomotionon rugged terrain: Theory and basic experiment," *Proc. Int. Conf. Advanced Robotics* (1991) pp. 741–746.
13. J. Yamaguchi, A. Takanishi and I. Kato, "Development of a biped walking robot adapting to a horizontally uneven surface," *Proc. IEEE/RSJ Int. Conf. Intelligent Robots and Systems*, Munich, Germany (Sep., 1994) pp. 1156–1163.
14. K. Hirai, M. Hirose, Y. Haikawa and T. Takenaka, "The development of honda humanoid robot," *Proc. IEEE Int. Conf. Robotics and Automation*, Leuven, Belgium (May 1998) pp. 1321–1326.
15. J. W. Cooley, P. A. Lewis and P. D. Welch, "The finite fourier transform," *IEEE Trans. of Audio and Electroacostics* **AU-17**, No. 2, 77–85 (1969).